

## Electronic structure of stannous oxide

M. Meyer<sup>a,\*</sup>, G. Onida<sup>b</sup>, A. Ponchel<sup>a</sup>, L. Reining<sup>a</sup>

<sup>a</sup> CNRS-CEA/DSM, Laboratoire des Solides Irradiés, Ecole Polytechnique, 91128 Palaiseau Cedex, France

<sup>b</sup> Dipartimento di Fisica, Università di Roma "Tor Vergata", I-00133 Rome, Italy

---

### Abstract

We present an ab initio study of the electronic structure of SnO. Density functional theory in the local density approximation (DFT-LDA) is used in conjunction with carefully tested smooth pseudopotentials. Total energies and charge densities are calculated and analysed as a function of the atomic geometry, with a particular emphasis on the importance of low-charge-density contributions to the interlayer cohesion. SnO<sub>2</sub> has already been studied in the past and is used for comparison. Copyright © 1998 Elsevier Science B.V.

*Keywords:* DFT-LDA; Oxide; Cohesion; Pseudo-potential

---

### 1. Introduction

Tin oxides are used in many fields of technological importance such as catalysis, chemical gas sensing, heat reflection and microelectronics. This is the reason for the numerous studies of their physical and chemical properties (including their electronic structure). Most of these investigations concern tin dioxide. However, stannous and stannic oxide coexist frequently due either to an oxygen loss associated with the reduction of SnO<sub>2</sub>, or to the oxidation of SnO.

The crystalline structures of SnO and SnO<sub>2</sub> are tetragonal at room temperature and normal pressure (Figs. 1(a) and (b)) and belong to space groups  $D_{4h}^7$  (P4/nmm) [1–3] and  $D_{4h}^{14}$  (P42/nmm), respectively. The oxidation process results mainly in the insertion of an oxygen plane between two tin planes in the layered SnO crystalline structure (see Figs. 1(c) and (d)).

As a result SnO<sub>2</sub> is a more densely packed crystal where each tin atom is surrounded by a slightly distorted oxygen octahedron while in SnO the tin atoms sit on the vertices of pyramids with an oxygen square basis (Fig. 1(b)). These edge sharing pyramids form the layers of the SnO structure with tin vertices lying alternately above and below them. The layers are stacked perpendicularly to the *c* crystallographic axis with tin atoms facing each other (Fig. 1(d)). In order to well understand the stability of this structure and the cohesion between its layers, it is important to have an accurate description of the atomic and electronic structure of SnO and of the relation between electronic and geometric configurations.

### 2. Methodology

Ab initio calculations using density functional theory (DFT) with the local density approximation

---

\* Corresponding author. Tel.: 33 1 69 45 01, fax: 33 1 69 33 30 22; e-Mail: Madeleine.Meyer@polytechnique.fr.

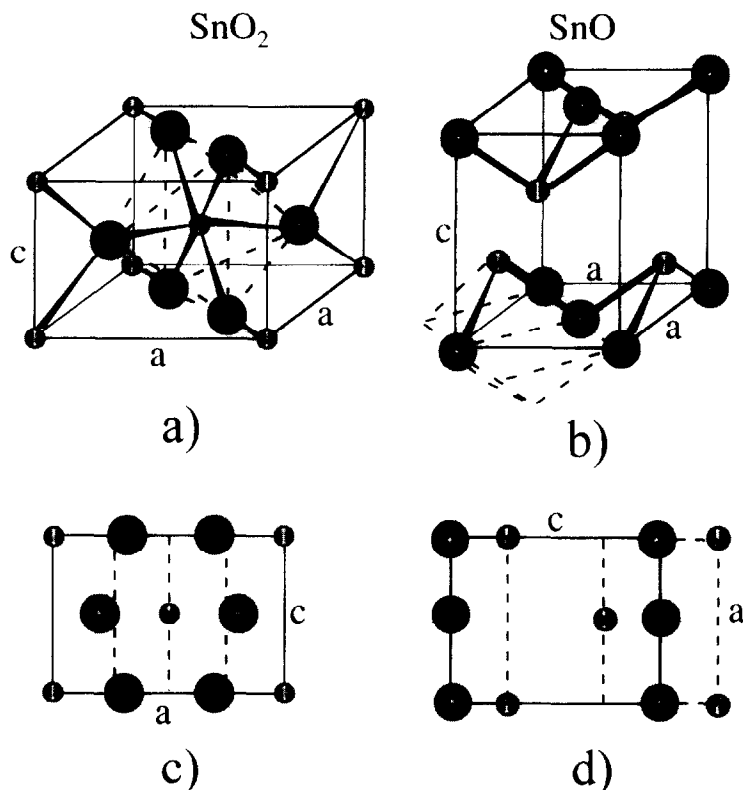


Fig. 1. Atomic configurations of  $\text{SnO}_2$  and  $\text{SnO}$ , the large spheres correspond to oxygen atoms and the smaller ones to tin atoms: (a) Structure of  $\text{SnO}_2$ : unit cell. The dashed lines link the O atoms forming an octahedron surrounding a tin atom. (b) Structure of  $\text{SnO}$ : unit cell. The dashed lines link the O atoms and the tin atom forming square-based pyramids. (c) Projection of the  $\text{SnO}_2$  unit cell onto a (100) plane showing the traces of the alternate O and Sn atomic planes. (d) Projection of the  $\text{SnO}$  unit cell onto a (010) plane showing the traces of the O and Sn atomic planes. An extra Sn plane has been added for the sake of comparison with (c).

(LDA) are performed in order to investigate the density of charge in  $\text{SnO}$  and its evolution with the atomic configuration. The Kohn Sham equations [4] are solved using the Car–Parrinello (CP) scheme [5] with normconserving pseudopotentials and a plane wave basis. This approach has been used with great success for various materials, but, in the case of oxides, the localised O 2p states require the use of a largely extended plane wave basis and consequently an important computational effort is necessary. The number of plane waves can be significantly reduced by the use of soft pseudopotentials [6] which have already proved to be efficient for oxides such as  $\text{TiO}_2$  [7],  $\text{SnO}_2$  [8] and  $\text{Li}_2\text{O}$  [9]. The oxygen soft pseudopotential created with a core cut-off radius of 1.45 a.u. allows us to get a good convergence of the total energy with

a kinetic energy cut-off equal to 70 Ry. A standard hard core norm conserving pseudopotential is used for the tin atoms [10] and the relative core contribution due to the 4d electrons is taken into account via a nonlinear core correction [11]. As usual with the CP method the Kleinman–Bylander (KB) separable form of the pseudopotential [12] is used with the p and d components as reference states for oxygen and tin, respectively. Eight  $\mathbf{k}$  points of the irreducible Brillouin zone are used to calculate the total energy of the electronic ground state associated with the atomic positions of tin and oxygen.

The unit cell of  $\text{SnO}$  contains two molecular units with atoms located as follows:  $\text{O}(000; 1/2\ 1/2\ 0)$ ,  $\text{Sn}(0\ 1/2\ u; 1/2\ 0\ \bar{u})$ . There are some discrepancies between the lattice parameters obtained by powder

X-ray data measurements ( $a = 3.796$  Å,  $c = 4.816$  Å,  $u = 0.2356$ ) [1] or neutron diffraction measurements ( $a = 3.799$  Å,  $c = 4.827$ ,  $u = ?$ ) [3]. The main uncertainty concerns the tin location since there is a significant lack of accuracy in the  $u$  determination. In our calculation the total energy is minimised, for each selected cell volume, with respect to the tin atom location ( $u$ ). The CP code allows us to take into account the symmetry of the forces and we apply for SnO a  $C_4$  symmetry around the  $c$  axis. This reduces the length of the calculations but keeps the atoms free to move in the  $[001]$  direction and allows for the determination of  $u$ . In order to determine the lattice constants that minimise the total energy, the calculations are performed for different values of the lattice parameters, in a range  $c = 4.0 - 4.827$  Å and  $a = 3.61 - 3.99$  Å.

### 3. Results and discussion

The 3D densities of charge calculated for SnO<sub>2</sub> and SnO at the experimental atomic configuration are plotted in Figs. 2 and 3(a). A simple look at the charge density distribution shows that the cohesion of SnO<sub>2</sub> is easy to understand. For SnO the explanation of the

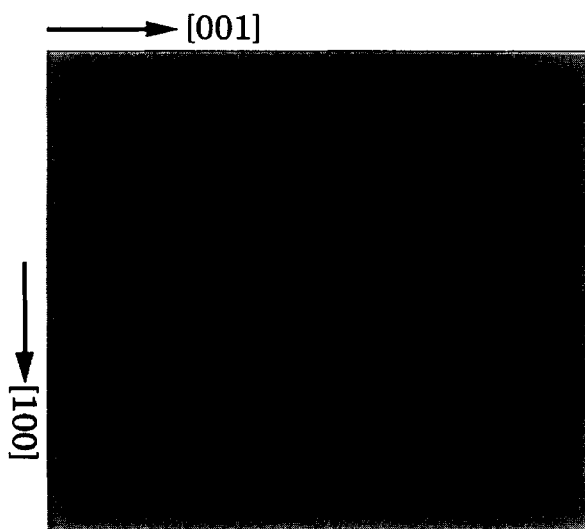


Fig. 2. 3D plot of the charge density calculated for the experimental configuration of SnO<sub>2</sub> ( $a = 4.74$  Å,  $c = 3.18$  Å,  $u = 0.307$ ), projection onto a  $(100)$  plane. Four isodensity surfaces are plotted. They correspond to the following values:  $5 \times 10^{-5}$ ,  $5 \times 10^{-4}$ ,  $2 \times 10^{-4}$ ,  $4 \times 10^{-4}$  electrons/(a.u.)<sup>3</sup>.

cohesion is not straightforward in terms of a description only involving the Madelung energy due to nominal charges. In fact, within the range of variation of  $c$ , the distance between tin atoms belonging to neighbouring layers is smaller than the Sn–O distance of atoms in second neighbour position (the O atoms first neighbours of Sn are located in the same layer). The layers should repel each other. The interatomic distances plotted in Fig. 4 show that when the structure is compressed in the  $c$  direction the Sn–Sn distance decreases less rapidly than the Sn–O second neighbour distance. Thus, the Sn–Sn repulsive interaction becomes more and more counterbalanced by the attractive Sn–O interlayers contribution. However, in this simple picture, the repulsive component remains dominant. A close look to the graphs of the densities of charge, plotted in Fig. 3, is necessary to understand the cohesion when  $c$  decreases. “Hats” of charge covering the Sn atoms appear which screen the Sn ions and decrease the repulsive forces, thus allowing for cohesion. This screening is hardly visible for the experimental value of  $c/a$  (Fig. 3(a)) and becomes more important when this ratio tends towards the value minimising the total energy (Fig. 3(d)).

A quantitative evaluation of the results shows however that our description of SnO contains some uncertainty. Our calculated values of the equilibrium lattice constants are  $a = 3.799$  Å, in very good agreement with experiment, and  $c = 4.286$  Å, which underestimates the most quoted experimental value of 4.827 Å by as much as 11%. No reliable experimental values are available for a comparison of  $u$ . The error in  $c$  is hence significantly higher than the few percent discrepancies which are typically found in LDA calculations.

We have checked that neither the particular choice of the pseudopotentials nor their KB form are responsible for this discrepancy. One might wonder about possible contributions of the 4d states of Sn, which have been treated as core states. They are in fact relatively close in energy to the oxygen 2s level. But first, the most important contribution of the Sn 4d electrons is the core-valence exchange, which is already taken into account by using a nonlinear core correction and second, the core relaxation effects are

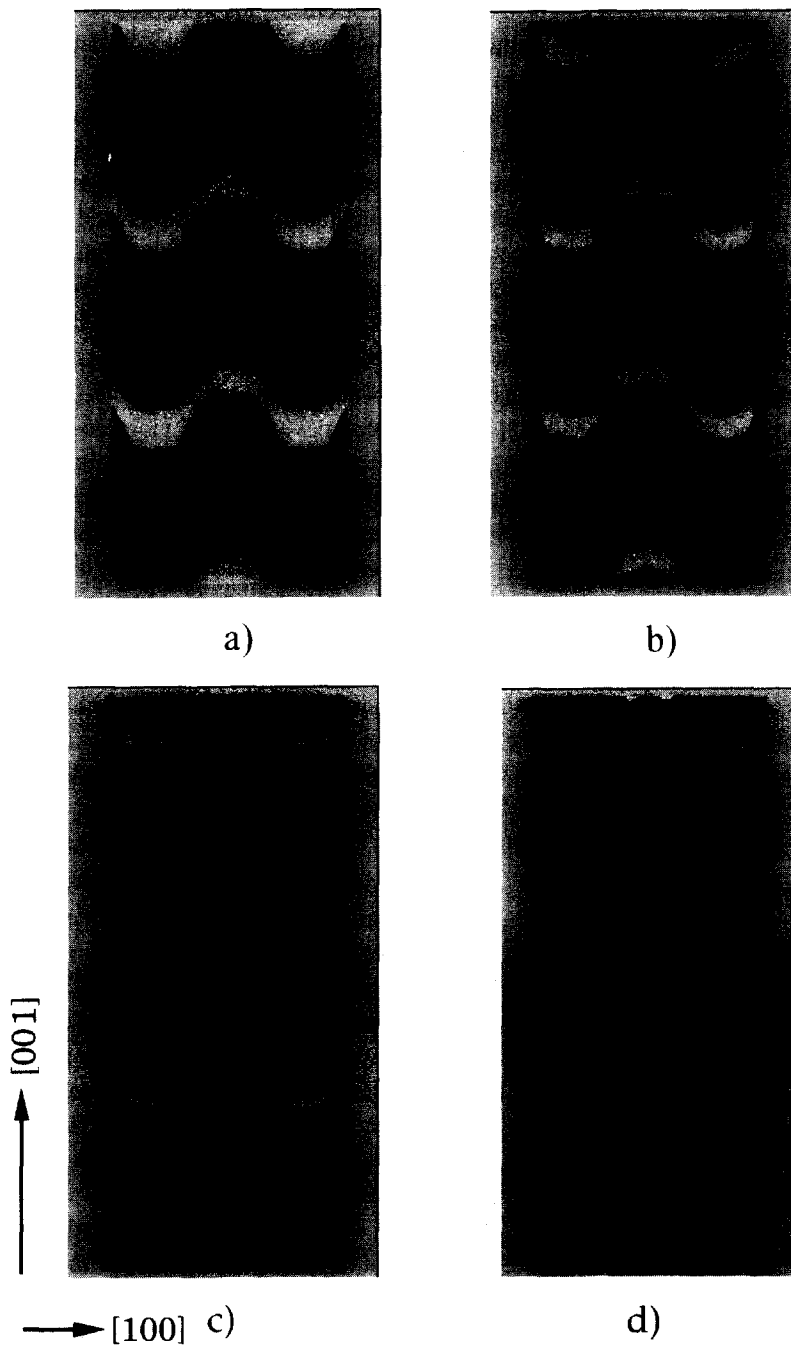


Fig. 3. 3D plot of the charge density of SnO obtained after total energy minimisation with a value of  $a = 3.799 \text{ \AA}$ : (a)  $c/a = 1.2706$  (experimental value); (b)  $c/a = 1.2$ ; (c)  $c/a = 1.15$ ; (d)  $c/a = 1.1074$  (minimum energy configuration). Projection onto a (010) plane. Four isodensity surfaces are plotted. They correspond to the following values:  $5 \times 10^{-5}$ ,  $5 \times 10^{-4}$ ,  $2 \times 10^{-4}$  and  $4 \times 10^{-4}$  electrons/(a.u.)<sup>3</sup>.

generally very small. It remains that the hybridisation of the Sn 4d with the O 2s levels could in principle give non-negligible modifications. However, calculations on SnO using localised basis sets and including the Sn 4d levels have explicitly shown that the Sn 4d states form a separate, narrow band and do not mix into the true valence states [13–14].

Since, as pointed out above by our qualitative discussion, the interlayer cohesion is due to a very delicate balance between ionic repulsion and screening, one could suspect particular difficulties linked to the LDA. They could be related to the fact that the LDA does not correctly cancel the electron self-interaction of the Hartree term, and hence underestimates the electron localisation. A smeared-out charge density between the layers would then be the consequence, with enhanced screening and hence overbinding. Although this hypothesis cannot be completely excluded, and may at least partially contribute to the observed behaviour, it is somehow contradicted by our charge density plots: the screening of the Sn atoms for small  $c/a$  ratios is in fact mostly due to the relatively localised “hats” on each Sn atom, and not to delocalised charge.

There is another point, however, which merits reflection. As in most standard CP codes, we have, as a first approach, used the d component of the pseudopotential as the local reference component for the Sn atom. This is in principle not recommended, since this component has been created with an excited configuration of the atom, and bears hence a bigger arbitrariness than the s and p components, which are created from the ground state [10]. Such a choice is nevertheless widely used, and generally does not lead to problems, apart from those which are indirectly linked to the KB separation through the remaining s and p non-local components. Bulk silicon, for example, does not show any visible difference when calculated with the p instead of the d component as local potential. In the case of SnO, however, more care seems to be needed. The equilibrium geometry is indeed extremely sensitive to a change in the reference component. The naïve solution would be to switch from the d to an s or p reference component. Unfortunately, this choice only worsens the results. This can be explained intuitively: the p (or s) potentials are

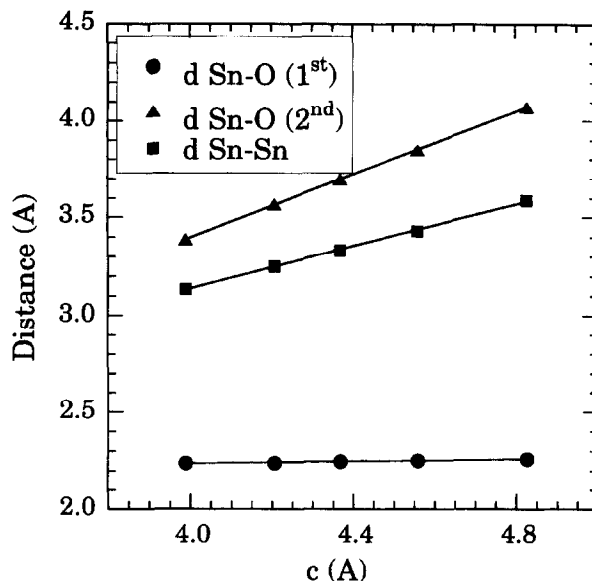


Fig. 4. Graph of the Sn–Sn and Sn–O distances plotted as a function of the  $c$  parameter. Two types of Sn–O distances are reported: the smaller ones (first neighbours) correspond to atoms belonging to the same layer, the larger ones correspond to atoms belonging to neighbouring layers.

more attractive than the d component. More charge is hence accumulated close to the Sn atoms, which means enhanced screening, which, in turn, leads to even smaller  $c/a$  values. This does actually happen; at constant  $a = 3.799$  Å, when using p as a reference state,  $c/a$  decreases again by more than 6% with respect to the value obtained with the d local potential. This implies that a reference component which is even less attractive than the d potential would be needed in order to get the results closer to experiment. In other words, the true potentials acting on higher angular components cannot be substituted in a satisfactory way by one of the lower components. This hypothesis is far from absurd, if one looks at the problem from the point of view of perturbation theory using a localised basis: in tin compounds, the Sn 4f states are more likely to contribute to the perturbed eigenstates than the 4f states of smaller atoms like silicon for example. One should hence expect that higher angular moments, in particular  $l = 3$ , are relatively important in tin oxides, and hardly allow a quick, approximate treatment. This problem is probably more pronounced

in SnO than in SnO<sub>2</sub>, because of the much more asymmetric geometry and charge distribution.

### Acknowledgements

This study has been supported by the scientific council of IDRIS/CNRS (France) through the allocation of computer time (project CP9/940127) and also in part by the European Community Program Human Capital and Mobility through contract no. ERB CHRX CT 930337.

### References

- [1] W.J. Moore, L. Pauling, *J. Am. Chem. Soc.* 63 (1941) 1392.
- [2] W.G. Wyckoff, *Crystal Structures*, 4th ed., Interscience, New York, 1974, p. 136.
- [3] D.M. Adams, A.G. Christy, J. Haines, *Phys. Rev. B* 46 (1992) 11 358.
- [4] W. Kohn, J.L. Sham, *Phys. Rev.* 140 (1965) A1133.
- [5] R. Car, M. Parrinello, *Phys. Rev. Lett.* 55 (1985) 2471.
- [6] N. Troullier, J.L. Martins, *Phys. Rev. B* 43 (1991) 1993.
- [7] K.M. Glassford, J.R. Chelikowsky, *Phys. Rev. B* 46 (1992) 1284.
- [8] M. Palumbo, L. Reining, M. Meyer, C.M. Bertoni, in: D.J. Lockwood (Ed.), *Proceedings of the 22nd ICPS, Vancouver, 1994*, World Scientific, Singapore, 1995, p. 161.
- [9] S. Albrecht, G. Onida, L. Reining, *Phys. Rev. B* 55 (1997) 10278.
- [10] G. Bachelet, D.R. Hamann, M. Schlüter, *Phys. Rev. B* 26 (1982) 4199.
- [11] S. Louie, S. Froyen, M. Cohen, *Phys. Rev. B* 26 (1982) 1738.
- [12] L. Kleinman, D.M. Bylander, *Phys. Rev. Lett.* 48 (1980) 1425.
- [13] J.M. Themlin, M. Chtaïb, L. Henrard, P. Lambin, J. Darville, J.M. Gilles, *Phys. Rev. B* 46 (1992) 2460.
- [14] J. Terra, D. Guenzburger, *Phys. Rev. B* 44 (1991) 8584.